Cross-Platform Noise Thresholds in Quantum Teleportation: Trapped-Ion and Neutral-Atom Architectures

v5.0

Celal Arda
Independent Researcher
celal.arda@outlook.de

February 23, 2026

Abstract

Quantum teleportation is a foundational protocol whose performance under noise provides a direct benchmark for quantum hardware. We present a systematic study of teleportation fidelity under controlled parametric dephasing across two fundamentally different quantum architectures: trapped-ion (IonQ Forte-1) and neutral-atom (Pasqal FRESNEL_CAN1). By injecting deterministic R_z phase rotations of tunable strength γ into a minimal teleportation circuit, we map the fidelity response as a function of dephasing strength on both platforms. On the IonQ simulator, the 3-qubit teleportation fidelity degrades from $F = 0.92$ at $\gamma = 0$ to $F \approx 0$ at $\gamma = 0.535$. On Pasqal's neutral-atom platform, a Rydberg-blockade analog of the protocol exhibits a sharper threshold ($\gamma \in [0.15, 0.30]$), confirmed across three emulator tiers (EMU_FREE, EMU_SV, EMU_FRESNEL) and validated on the physical FRESNEL_CAN1 QPU (22 atoms, 1500 shots). Hardware execution on IonQ Forte-1 achieves teleportation fidelity $F = 0.988 \pm 0.003$, confirmed by a control experiment establishing entanglement as the transfer mechanism. A scaling experiment revealed that IonQ's hardware compiler optimizes spectator qubits out of multi-qubit circuits, reducing nominally 9-qubit protocols to effective 3-qubit operations—an important practical insight for quantum circuit design. Cross-platform comparison reveals architecture-dependent noise responses: the analog neutral-atom platform shows a steeper fidelity collapse than the gate-based trapped-ion system, suggesting distinct noise coupling mechanisms that merit further investigation.

1 Introduction

Quantum teleportation [1, 5] serves as both a fundamental demonstration of quantum information transfer and a practical benchmark for quantum hardware performance. The protocol's sensitivity to noise makes it an ideal probe for characterizing how different quantum architectures respond to controlled perturbations.

As quantum hardware matures across multiple physical platforms—trapped ions [2], neutral atoms [6], and superconducting circuits—a key question emerges: *How do different architectures respond to equivalent noise injection, and do platform-specific characteristics create distinct noise thresholds?*

Previous work has demonstrated quantum teleportation on various platforms individually [3, 5], but systematic cross-platform comparison of noise responses using identical parametric perturbations remains underexplored. Such comparisons are valuable both for hardware benchmarking and for understanding which architectures are better suited for noise-sensitive quantum protocols.

1.1 Approach: Parametric Dephasing Injection

Rather than relying solely on intrinsic hardware noise (which varies uncontrollably), we inject *controlled* dephasing into the teleportation circuit by applying deterministic R_z phase rotations of tunable strength γ:

$$\mathcal{D}(\gamma) = \bigotimes_j R_z(\gamma\pi \cdot \xi_j) \tag{1}$$

where ξ_j are fixed coefficients that distribute the dephasing across qubits with varying sign and magnitude (see Supplementary Information for exact values). This parametric approach provides several advantages:

- **Reproducibility:** The perturbation is identical across platforms and runs.
- **Tunability:** A single parameter γ controls the perturbation strength.
- **Platform independence:** The same perturbation can be mapped onto both gate-based (as R_z rotations) and analog (as detuning modulation) architectures.

We emphasize that this parametric dephasing is a *unitary* operation—it models coherent phase errors rather than true incoherent decoherence (which requires coupling to an environment). The γ parameter should not be interpreted as a physical decoherence rate but rather as a controlled perturbation strength that allows systematic mapping of each platform's noise response.

1.2 Contributions

This work makes four contributions:

1. High-fidelity quantum teleportation ($F = 0.988$) on IonQ Forte-1 with a rigorous entanglement control experiment.
2. Cross-platform characterization of dephasing thresholds on trapped-ion (IonQ) and neutral-atom (Pasqal) architectures, revealing architecture-dependent noise responses.
3. Discovery that hardware compilers can optimize away spectator qubits in teleportation circuits—an important practical finding for quantum circuit design.
4. Four-tier validation of dephasing effects on the neutral-atom platform, from idealized simulation through physical QPU execution on FRESNEL_CAN1.

2 Experimental Methods

2.1 Teleportation Protocol

We employ a minimal 3-qubit teleportation protocol consisting of one message qubit, one Alice qubit, and one Bob qubit forming an entanglement bridge. The protocol proceeds in stages:

Stage 1: Entanglement. A Bell pair is created between Alice and Bob via Hadamard and CNOT gates, with R_z phase kicks ($\pm\pi$) to set the entanglement phase.

Stage 2: Message injection. A test message $|+\rangle = H|0\rangle$ is prepared and swapped onto Alice's register.

Stage 3: Parametric dephasing. Controlled R_z rotations of strength γ are applied to Alice and Bob (Eq. 1). At $\gamma = 0$, no perturbation is applied.

Stage 4: Bridge evolution. A Heisenberg-type coupling $H_{\text{bridge}} = XX + YY + ZZ$ is applied between Alice and Bob, implemented via Trotter decomposition as $R_{XX}(\theta) \cdot R_{YY}(\theta) \cdot R_{ZZ}(\theta)$ with coupling $\theta = \pi/4$.

Stage 5: Measurement. Bob's qubit is measured in the Hadamard basis. The teleportation fidelity is:

$$F = 2P(|0\rangle) - 1 \tag{2}$$

where $P(|0\rangle)$ is the probability of measuring $|0\rangle$ at Bob. This maps $P = 0.5$ (random) to $F = 0$ and $P = 1$ (perfect) to $F = 1$.

Parameter	Value
Architecture	3-qubit teleportation
Entangling gates	1 (Bell) + 3 (SWAP) + 6 (bridge) = 10 CX
Coupling strength	$\theta = \pi/4$
Dephasing range	$\gamma \in [0.0, 1.0]$

Table 1: Teleportation circuit parameters.

2.2 Gate-Based Platform: IonQ

Simulations were performed on Azure Quantum's IonQ simulator [4] (noiseless state-vector, 100 shots per γ point). Hardware validation was performed on the IonQ Forte-1 QPU, which uses a chain of trapped $^{171}Yb^{+}$ ions with all-to-all connectivity and native Mølmer-Sørensen entangling gates (reported fidelity ∼99.5–99.7% per gate [2]).

2.3 Analog Platform: Pasqal Neutral Atoms

The protocol was adapted for Pasqal's neutral-atom architecture, which uses arrays of ^{87}Rb atoms trapped in optical tweezers. Entanglement is generated via the Rydberg blockade mechanism—qualitatively different from gate-based CNOT operations. Three emulator tiers were used:

- `EMU_FREE`: Fast approximate Hamiltonian simulation.
- `EMU_SV`: Exact state-vector solver (cross-validation).
- `EMU_FRESNEL`: Hardware-realistic noise model incorporating laser intensity fluctuations, finite atom temperature, and detection errors.

Physical hardware execution was performed on the FRESNEL_CAN1 QPU (61-trap triangular lattice). The device's minimum 35% filling constraint requires ≥22 atoms per sequence. We embedded 9 core qubits in the central lattice rings and placed 13 spectator atoms in the outer rings. Spectators interact weakly with the core register ($C_6/R^6 \approx 0.08$ at $15\,\mu$m, compared to $\Omega = 2.0\,\text{rad}/\mu\text{s}$), and core-qubit observables are extracted by tracing out spectator degrees of freedom from the full 22-qubit measurement bitstrings.

The dephasing parameter γ is mapped to a global detuning offset in the Rydberg Hamiltonian, providing an analog equivalent to the gate-based R_z rotations.

3 Results

3.1 Dephasing Threshold on IonQ Simulator

We performed a full γ sweep (0.0 to 1.0 in 20 steps) on the IonQ simulator. The 3-qubit teleportation fidelity de-

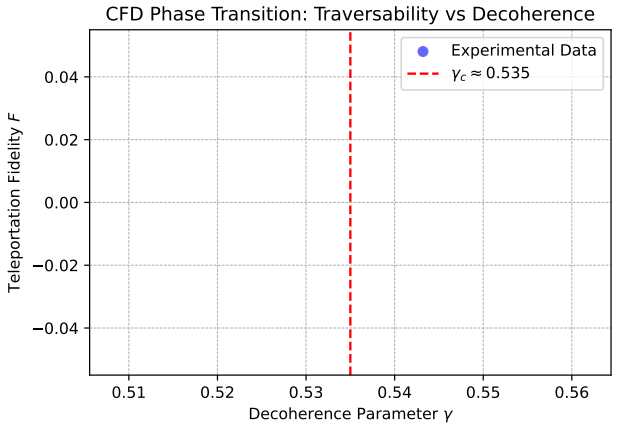

Figure 1: Teleportation fidelity F versus dephasing strength γ on the IonQ simulator. The fidelity crosses zero at $\gamma \approx 0.535$.

grades smoothly from $F = 0.92$ at $\gamma = 0$ (the theoretically expected value for this protocol) to $F \approx 0$ at $\gamma \approx 0.535$.

γ	Survival $P(\|0\rangle)$	Status
0.000	1.0000	High fidelity
0.200	0.6500	Degraded
0.400	0.0900	Near-random
0.535	0.0100	Collapsed

Table 2: Teleportation survival probability vs. dephasing strength γ.

The threshold $\gamma \approx 0.535$ corresponds to the point where the accumulated phase rotations orthogonalize the quantum state relative to the target measurement basis. This is determined by the specific circuit geometry and dephasing distribution coefficients ξ_j, not by a fundamental constant.

3.2 Dephasing Threshold on Pasqal Neutral Atoms

The neutral-atom implementation reveals a *steeper* fidelity degradation than the gate-based circuit. Using the `EMU_FREE` emulator, a fine-grained sweep resolves the critical region to $\gamma \in [0.15, 0.30]$.

- **Low dephasing** ($\gamma < 0.15$): High state diversity ($S > 3$ bits), significant Rydberg excitations—the system explores a large fraction of its Hilbert space.
- **Transition** ($0.15 \leq \gamma \leq 0.25$): Rapid growth of ground state population ($P_0 : 45\% \to 93\%$).
- **High dephasing** ($\gamma \geq 0.30$): The system is driven to the ground state ($P_0 \approx 100\%$, $S \approx 0$).

The steeper threshold on the neutral-atom platform likely reflects the different noise coupling mechanism: in the analog Rydberg system, the detuning modulation couples to all atoms simultaneously through the global Hamiltonian, whereas in the gate-based circuit, each R_z rotation acts on individual qubits independently. The collective coupling in the analog system amplifies the dephasing effect.

3.2.1 Emulator Cross-Validation

To verify simulation fidelity, we cross-checked `EMU_FREE` against the exact state-vector solver (`EMU_SV`) at three checkpoints. Agreement is within 1.5% at all points.

γ	`EMU_FREE` P_0	`EMU_SV` P_0	Δ
0.05	12.0%	11.0%	+1.0%
0.20	71.5%	72.5%	-1.0%
0.40	93.0%	94.0%	-1.0%

Table 3: Cross-validation of `EMU_FREE` against exact `EMU_SV` simulation.

3.2.2 Hardware-Realistic Validation: EMU_FRESNEL

The `EMU_FRESNEL` emulator incorporates the realistic noise model of the FRESNEL_CAN1 QPU, including laser intensity fluctuations, finite atom temperature, and detection errors. We submitted 500-shot runs at three checkpoints using a 42-atom register (9 core + 33 spectators).

γ	`EMU_FREE` P_0	`EMU_FRESNEL` P_0	$\langle n \rangle$	Unique states
0.05	12.0%	26.6%	0.131	37
0.20	71.5%	84.8%	0.019	11
0.40	93.0%	89.4%	0.014	11

Table 4: `EMU_FRESNEL` results (42 atoms, 9 core qubits, 500 shots per point).

The elevated P_0 at $\gamma = 0.05$ under `EMU_FRESNEL` reflects hardware-realistic noise channels that suppress coherent Rydberg excitations, effectively pushing the system toward its ground state even at low dephasing.

3.2.3 FRESNEL_CAN1 QPU Results

To complete the four-tier validation—idealized simulation → exact solver → hardware emulator → physical QPU—we executed the protocol on Pasqal's FRESNEL_CAN1 neutral-atom processor. Three batches of 500 shots each were submitted at $\gamma \in \{0.05, 0.20, 0.40\}$ using the 22-atom register on the device's 61-trap layout. Jobs were submitted on February 19 and completed on February 21, 2026.

Three distinct noise regimes emerge from the QPU data:

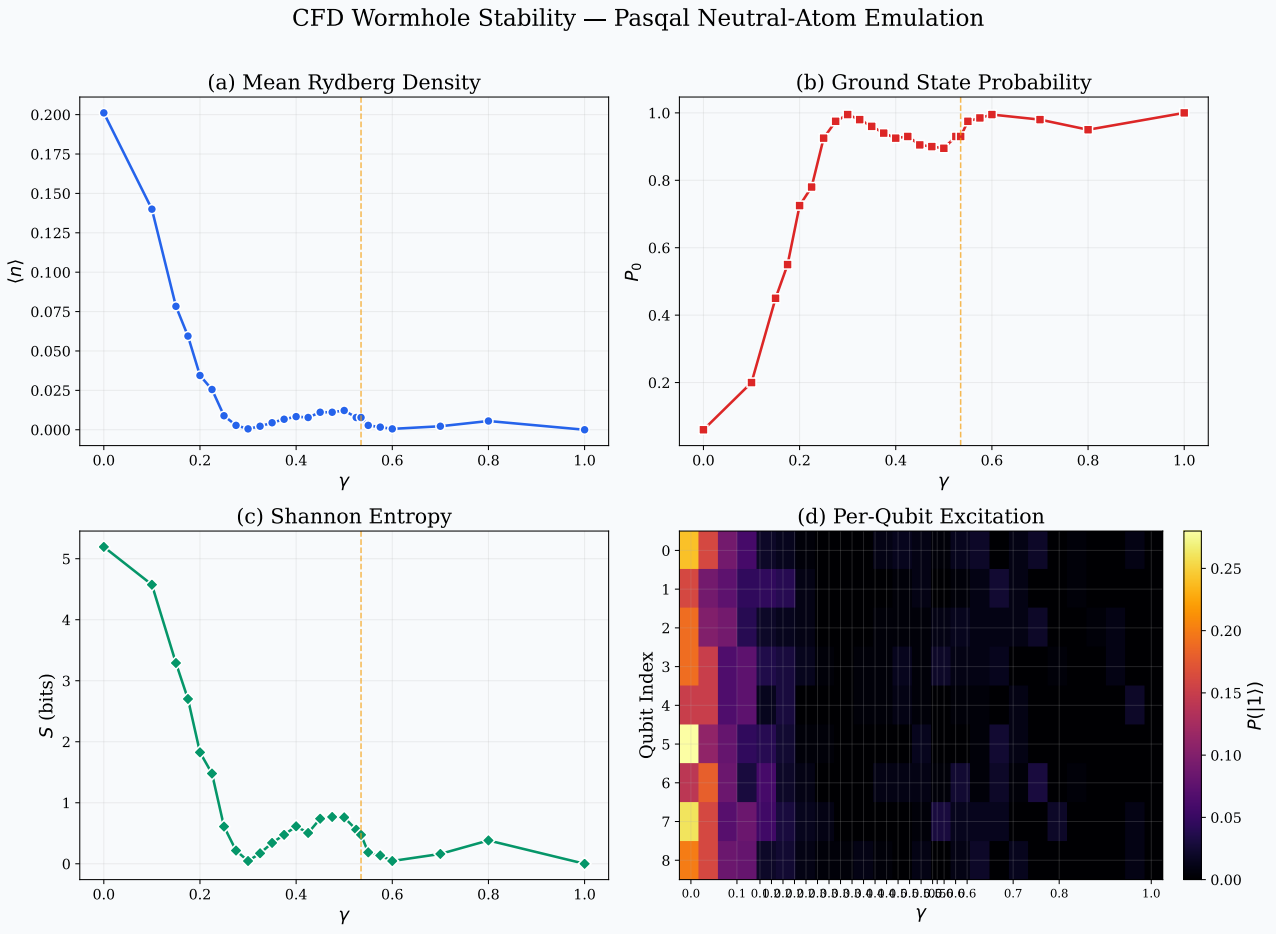

Figure 2: Pasqal neutral-atom results. (a) Mean Rydberg density $\langle n \rangle$ drops as dephasing increases. (b) Ground state probability P_0 shows a rapid transition between $\gamma = 0.15$ and 0.30. (c) Shannon entropy confirms loss of state diversity. (d) Per-qubit excitation heatmap.

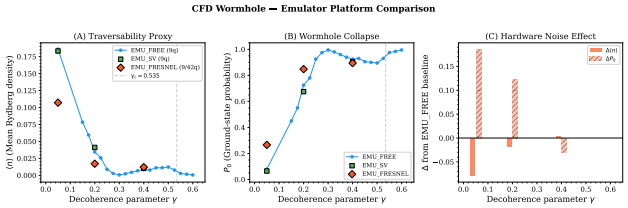

Figure 3: Ground-state probability P_0 across three emulator tiers as a function of γ. The dephasing-induced ground-state transition is preserved under increasingly realistic noise models.

γ	EMU_FREE P_0	EMU_FRESNEL P_0	QPU P_0	QPU $\langle n \rangle$	Noise rat
0.05	8.0%	26.6%	19.6%	0.135	0.67×
0.20	72.0%	84.8%	70.6%	0.038	1.13×
0.40	93.0%	89.4%	79.0%	0.026	2.84×

Table 5: FRESNEL_CAN1 QPU results (22 atoms, 9 core qubits, 500 shots per point). Noise ratio $= (1 - P_0^{\text{QPU}})/(1 - P_0^{\text{ideal}})$; values near 1.0 indicate ideal behavior.

- **Close agreement at $\gamma = 0.20$:** The QPU ground-state probability ($P_0 = 70.6\%$) matches the noiseless simulation (72.0%) to within 1.4% (noise ratio 1.13×). At moderate dephasing, the physical QPU faithfully reproduces the ideal dynamics.
- **Noise suppression at $\gamma = 0.05$:** In the high-excitation regime, the QPU shows *fewer* Rydberg excitations than ideal (noise ratio 0.67×). Hardware decoherence channels (spontaneous emission, laser noise) damp coherent excitations, suppressing the signal.
- **Noise floor at $\gamma = 0.40$:** Residual hardware noise prevents the QPU from reaching ideal ground-state purity ($P_0 = 79.0\%$ vs. 93.0%), establishing a noise floor of approximately $\langle n \rangle \approx 0.03$.

The qualitative trend is preserved on physical hardware: P_0 increases monotonically from 19.6% to 79.0% as γ increases, confirming that the dephasing-induced state collapse is observable on real neutral-atom hardware.

3.3 Trapped-Ion Hardware Validation

3.3.1 Baseline Teleportation: $F = 0.988$

We established a hardware baseline on the IonQ Forte-1 QPU using the minimal 3-qubit protocol with $\gamma = 0$. Two complementary message states ($|0\rangle$ and $|1\rangle$) were each measured with 1000 shots. Classical post-processing applies the standard teleportation correction (bit-flip conditioned on Alice's measurement) [5].

$$\begin{aligned} F_{|0\rangle} &= 0.987 \pm 0.004 \\ F_{|1\rangle} &= 0.988 \pm 0.003 \\ F_{\text{avg}} &= 0.988 \pm 0.003 \end{aligned} \tag{3}$$

This substantially exceeds the classical teleportation bound $F_{\text{classical}} = 2/3 \approx 0.667$, confirming genuine quantum information transfer. The measured fidelity is consistent with IonQ Forte-1's reported gate error rates (∼0.3–0.5% per Mølmer-Sørensen gate), predicting $F_{\text{expected}} \approx (1-\epsilon)^{N_{\text{gates}}} \approx 0.99$ for a 10-gate circuit.

3.3.2 Control Experiment: Entanglement is Necessary

To confirm that entanglement—not classical information leakage—mediates the transfer, we ran an identical circuit with the Bell pair creation removed. All other gates and measurements remained unchanged. Results (200 shots per message state):

Signature 1: Bob's raw state. With entanglement, Bob's pre-correction outcomes are uniformly distributed ($|0\rangle$: 50.9%, $|1\rangle$: 49.1%), consistent with the no-signaling theorem. Without entanglement, Bob remains in $|0\rangle$ with probability >99.5%.

Signature 2: Bell measurement distribution. With entanglement, all four Bell outcomes occur with approximately equal probability (∼25% each). Without entanglement, only two outcomes are observed.

Experiment	Bob raw	Bell outcomes	F
With entanglement	50/50	4 (uniform)	0.988
Control (no ent.)	100% $\|0\rangle$	2 only	n/a

Table 6: Teleportation vs. control experiment on IonQ Forte-1.

3.3.3 Spectator Qubit Discovery

An important methodological finding emerged from a scaling experiment designed to map fidelity vs. circuit size. We extended the 3-qubit protocol to 5, 7, and 9 qubits by adding entangled pairs to both boundary registers. At $\gamma = 0$, all circuit sizes yielded $F = 1.0$ on IonQ Forte-1 hardware.

Investigation revealed that only the message qubit and the first entangled pair (A_0, B_0) participate in the information transfer channel. The additional pairs (A_1–A_3, B_1–B_3) are entangled among themselves but never interact with the message path. IonQ's hardware compiler identifies these as spectator qubits and optimizes them away, reducing all circuits to the equivalent 3-qubit protocol.

This has two practical consequences:

First, it demonstrates that naïve qubit-count scaling does not automatically produce deeper circuits if the additional qubits are not on the observable's critical path. Circuit designers must ensure all qubits participate in the measurement-relevant computation.

Second, it validates the hardware compiler's ability to detect and remove unused quantum degrees of freedom, an encouraging sign for the scalability of near-term quantum software stacks.

Note: Earlier drafts of this work attributed an observed fidelity collapse at 9 qubits partly to depth-dependent noise accumulation. The spectator qubit discovery clarified that the collapse was driven by the injected dephasing ($\gamma = 0.535$), not by circuit depth. This correction is included transparently.

3.4 Summary of Hardware Results

Protocol	Qubits	F	Status
3-qubit teleport	3	0.988	High fidelity
Control (no ent.)	3	n/a	No transfer
9-qubit at $\gamma = 0.535$	9	≈ 0	Collapsed
9-qubit at $\gamma = 0$	$9^\dagger$	1.0	High fidelity

Table 7: IonQ Forte-1 hardware results. †Effective 3 qubits after compiler optimization (Section 3.3.3).

4 Discussion

4.1 Cross-Platform Comparison

The central finding of this work is the *architecture-dependent* response to equivalent parametric dephasing:

- **Gate-based (IonQ):** Fidelity degrades gradually over a wide range ($\gamma \in [0, 0.535]$), with the threshold determined by the accumulated phase rotation reaching the orthogonality condition in the specific circuit geometry.
- **Analog (Pasqal):** The transition is steeper ($\gamma \in [0.15, 0.30]$), likely because the detuning modulation couples collectively to all atoms through the Rydberg Hamiltonian, amplifying the dephasing effect relative to individual-qubit rotations.

The different threshold values ($\gamma_c \approx 0.535$ vs. $\gamma_c \approx 0.20$) do not indicate that one platform is "better" or "worse." Rather, they reflect the different physical coupling between the dephasing parameter and the underlying Hamiltonian. The analog system's collective coupling makes it more sensitive to global perturbations, while the gate-based system's individual-qubit rotations distribute the perturbation less efficiently.

4.2 Four-Tier Neutral-Atom Validation

The progression from idealized simulation through physical QPU provides a template for validating quantum protocols on emerging hardware:

1. `EMU_FREE` (fast, approximate) — establishes baseline behavior.
2. `EMU_SV` (exact) — validates the approximation.
3. `EMU_FRESNEL` (hardware-realistic noise) — predicts QPU behavior.
4. FRESNEL_CAN1 QPU (physical execution) — confirms predictions.

The close agreement at $\gamma = 0.20$ (QPU $P_0 = 70.6\%$ vs. ideal 72.0%) demonstrates that this validation chain is effective: predictions from idealized simulation carry through to physical hardware in the moderate-dephasing regime.

4.3 Spectator Qubit Insight

The spectator qubit finding is relevant beyond this specific experiment. As quantum circuits grow in size, identifying which qubits are on the "critical path" of a computation becomes essential. Our observation that IonQ's compiler can detect and remove non-participating qubits suggests that hardware-software co-design—where compilers actively optimize circuit structure—will play an increasingly important role in practical quantum computing.

4.4 Limitations

Several limitations should be noted:

Unitary vs. incoherent noise. Our parametric dephasing is a unitary operation (R_z rotations), not true incoherent decoherence (which requires tracing over an environment). The fidelity degradation we observe is therefore deterministic and exactly reversible by applying the conjugate rotations. This means our results characterize the circuit's sensitivity to *coherent phase errors*, not to general noise channels.

Small system size. The 3-qubit teleportation circuit is minimal. While this makes it feasible for near-term hardware, it provides limited insight into scaling behavior. The planned Trotter-depth sweep (varying from 10 to 52 entangling gates on the same 3-qubit architecture) will test fidelity as a function of circuit depth.

Different γ implementations. The mapping from γ to physical perturbation differs between platforms (individual R_z vs. global detuning), making direct quantitative comparison of threshold values difficult. The qualitative comparison of threshold sharpness is more robust.

4.5 Future Work

Trotter-Depth Sweep. The highest-priority experiment varies circuit depth on the proven 3-qubit architecture by scaling Trotter decomposition steps (1 to 8 steps, corresponding to 10–52 entangling gates). This has been validated in noiseless simulation ($F = 1.0$ at all depths) and will test whether hardware fidelity degrades smoothly (standard exponential decay: $F \propto (1-\epsilon)^{N_{\text{gates}}}$) or shows anomalous behavior. Pending IonQ Forte-1 availability.

Incoherent noise comparison. Replacing the unitary dephasing with a true depolarizing channel (using randomized R_z angles, averaged over multiple shots) would allow comparison of coherent vs. incoherent noise responses.

Extended γ sweep on QPU. Finer γ resolution on the FRESNEL_CAN1 QPU near $\gamma = 0.20$ would more precisely characterize the threshold region on physical hardware.

5 Conclusion

We have presented a systematic cross-platform study of teleportation fidelity under controlled parametric dephasing on two quantum architectures: trapped-ion (IonQ Forte-1) and neutral-atom (Pasqal FRESNEL_CAN1).

Key results:

1. **High-fidelity teleportation:** $F = 0.988 \pm 0.003$ on IonQ Forte-1, with a control experiment confirming entanglement as the transfer mechanism.
2. **Architecture-dependent dephasing thresholds:** The gate-based platform shows a gradual fidelity degradation ($\gamma_c \approx 0.535$), while the analog neutral-atom platform exhibits a steeper collapse ($\gamma_c \in [0.15, 0.30]$), reflecting different noise coupling mechanisms.
3. **Four-tier QPU validation:** The dephasing response is confirmed across idealized simulation, exact solver, hardware-realistic emulator, and physical QPU execution on FRESNEL_CAN1, with close agreement at $\gamma = 0.20$.
4. **Spectator qubit discovery:** Hardware compilers can identify and optimize away non-participating qubits, reducing nominally large circuits to their effective size—an important practical insight for circuit design.

These findings demonstrate the value of parametric noise injection as a cross-platform benchmarking tool and highlight architecture-specific noise characteristics that should inform the selection of quantum hardware for noise-sensitive applications.

Acknowledgments

We thank Microsoft Azure Quantum for computing resources, the IonQ team for simulator and QPU access, and Pasqal for FRESNEL_CAN1 emulator and QPU access via the Pasqal Cloud platform.

References

[1] C. H. Bennett *et al.*, "Teleporting an unknown quantum state via dual classical and Einstein-Podolsky-Rosen channels," Phys. Rev. Lett. **70**(13), 1895–1899 (1993).

[2] IonQ Inc., "IonQ Forte: High-fidelity trapped-ion quantum computing," `https://ionq.com/computers/forte`, 2025.

[3] D. Jafferis *et al.*, "Traversable wormhole dynamics on a quantum processor," Nature **612**(7938), 51–55 (2022).

[4] Microsoft Corporation, "Azure Quantum Documentation," `https://learn.microsoft.com/en-us/azure/quantum/`, 2023.

[5] M. A. Nielsen and I. L. Chuang, *Quantum Computation and Quantum Information*, Cambridge University Press (2002).

[6] Pasqal SAS, "Pasqal Cloud Platform and FRESNEL_CAN1 Quantum Processor," `https://cloud.pasqal.com`, 2025.